Research article

Victor Pacheco-Peña and Nader Engheta*

Effective medium concept in temporal metamaterials

https://doi.org/10.1515/nanoph-2019-0305
Received August 6, 2019; revised October 27, 2019; accepted November 2, 2019

Abstract: Metamaterials are mostly designed in the time-harmonic scenario where wave propagation can be spatially manipulated. Tailoring the electromagnetic response of media in time has also gained the attention of the scientific community in order to achieve further control on wave-matter interaction both in space and time. In the present work, a temporally effective medium concept in metamaterial is theoretically investigated as a mechanism to create a medium with a desired effective permittivity. Similar to spatially subwavelength multilayered metamaterials, the proposed "temporal multilayered", or "multistepped" metamaterial, is designed by alternating in time the permittivity of the medium between two values. In so doing, the temporally periodic medium can be modeled as an effective metamaterial in time with an effective permittivity initiated by a step function. The analogy between the temporal multistepped and the spatial multilayered metamaterials is presented demonstrating the duality between both domains. The proposed temporal metamaterial is analytically and numerically evaluated showing an excellent agreement with the designed parameters. Moreover, it is shown how the effective permittivity can be arbitrarily tailored by changing the duty cycle of the periodic temporal metamaterial. This performance is also connected to the spatial multilayer scenario in terms of the filling fraction of the different materials used to create the multilayered structures.

Keywords: temporal metamaterials; effective medium; multilayered media; metamaterials.

***Corresponding author: Nader Engheta,** Department of Electrical and Systems Engineering, University of Pennsylvania, Philadelphia, PA 19104, USA, e-mail: engheta@ee.upenn.edu.
https://orcid.org/0000-0003-3219-9520
Victor Pacheco-Peña: School of Engineering, Newcastle University, Merz Court, Newcastle Upon Tyne NE1 7RU, UK.
https://orcid.org/0000-0003-2373-7796

1 Introduction

The arbitrary control of wave-matter interaction by spatially designing the electromagnetic properties of media has been of great interest within the research community for decades [1]. Within this context, metamaterials [and metasurfaces as their two-dimensional (2D) version] have been studied and demonstrated at different spectral ranges such as microwave, terahertz, and optics [2–11] achieving extreme parameters of permittivity (ε) and permeability (μ) such as near-zero or negative [12–19]. Metamaterials have opened new paths to tailor and engineer wave propagation at will giving rise to new and improved applications such as sensors [20–22], antennas [23–27], beam shaping, [28–30] and mathematical operators [31], to name a few.

Since their conception, metamaterials and metasurfaces have been mostly studied within the time-harmonic scenario (frequency domain). In this realm, wave-matter interaction is controlled by properly engineering the electromagnetic properties of media in space (i.e. along the x, y, z coordinates). However, to further control wave propagation at will, there is another dimension, time (t), that can be manipulated in addition to these three dimensions. Space-time metamaterials have been studied since several decades ago [32, 33] and they have recently been used for exciting applications [34, 35] such as inverse prism [36], frequency conversion [37], nonreciprocity [38–40], temporal band-gap, and time reversal [41–48]. The idea of "time crystals" has also been introduced and developed [49–52].

Inspired by the broad opportunities offered by spatial and temporal modulated metamaterials, in this work we investigate (and demonstrate both analytically and numerically) a mechanism to achieve a temporally effective permittivity using temporal metamaterials. As well known in the spatial case (time-harmonic scenario), metamaterials with effective permittivity can be designed by alternating subwavelength layers of different materials in a periodic fashion [14, 53–56]. Here, the temporal version of such spatial multilayered metamaterial

is considered by modulating the permittivity of the medium in time. Similar to the spatial case, the "multilayered" or multistepped temporal effective medium is designed by changing the permittivity of the whole medium from ε_1 to ε_2 and returning to ε_1 with a periodicity much smaller than the period of the incident wave. By doing so, the multistepped temporal metamaterial is able to emulate an effective permittivity as if the permittivity was changed in time following a step function. The similarities and differences between the spatial and temporal multilayered effective metamaterials are presented here. The effect of the periodicity and duty cycle of the time-dependent permittivity for the temporal version of multilayered metamaterials is also evaluated, demonstrating that the resulting effective permittivity can be tailored when changing the duty cycle of the temporal change. All the designs studied here were numerically evaluated using the time-domain solver of the commercial software COMSOL Multiphysics®.

2 Theory and results

2.1 Connection between spatial multilayers and temporal multisteps

To begin with, let us consider the well-known spatial multilayered structure shown in Figure 1A. It consists of periodically arranged layers of two different materials (with permittivity ε_1 and ε_2, both assumed to be real positive quantities) along the propagation z-axis. The different layers are considered to be infinitely extent along the x and y directions with thicknesses much smaller than the incident wavelength in each medium. The resulting structure is illuminated with a plane wave under normal incidence. As described in the introduction, it is well known in the conventional effective medium theory in electromagnetics [56] that such spatial multilayered structures can be used to create metamaterials with an anisotropic

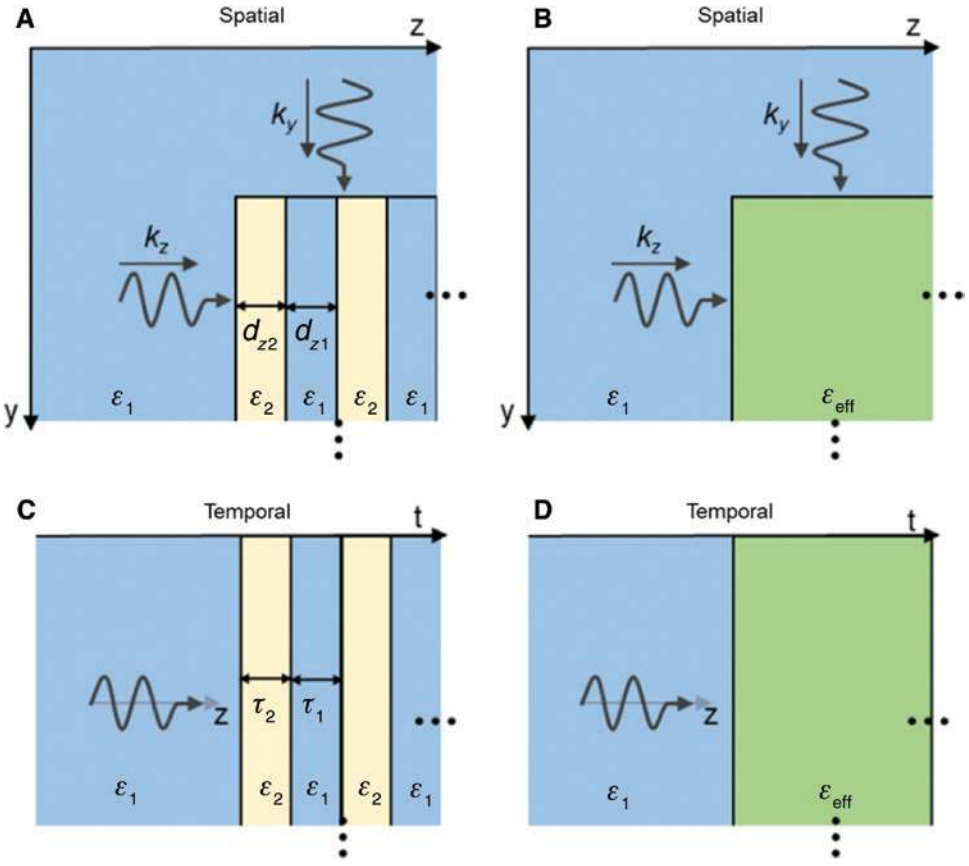

Figure 1: Schematic representation of the spatial and temporal multilayered metamaterials and their corresponding effective media. Top row: Schematic representation of a well known spatial multilayered structure made with alternating subwavelength layers of two media with different permittivity ε_1 and ε_2 (A), along with the effective medium produced by such spatial multilayered medium (B). Bottom row: Schematic representation of the temporal analogue, i.e. the proposed multistepped temporal metamaterial made by alternating in time subperiod steps of two different permittivities ε_1 and ε_2 (C), along with the temporally effective medium produced by such temporal multistepped medium (D).

effective permittivity $\boldsymbol{\varepsilon}_{\mathbf{eff}}$ (ε_{effxx}, ε_{effyy}, ε_{effzz}, for polarization of the E field along the *x*, *y* and *z* axis, respectively) as symbolically shown in Figure 1B. In this scenario, the ε_{eff} in each spatial coordinate depends on the values of ε_1 and ε_2 as well as the thickness of each layer. Based on this, the ε_{eff} for the spatial multilayered metamaterial can be expressed as follows [56–58]:

$$\varepsilon_{effxx} = \varepsilon_{effyy} = \varepsilon_1(1-\Delta_{z2}) + \Delta_{z2}\varepsilon_2 \tag{1a}$$

$$\varepsilon_{effzz} = \frac{\varepsilon_1\varepsilon_2}{\varepsilon_1\Delta_{z2} + \varepsilon_2(1-\Delta_{z2})} \tag{1b}$$

where $\Delta_{z1} = 1-\Delta_{z2}$ and Δ_{z2} are the filling fractions for each subwavelength layer (ε_1 and ε_2, respectively) defined as the ratio between the absolute thicknesses of each layer with respect to the total thickness of one spatial period $\Delta_{z1,2} = d_{z1,2}/(d_{z1}+d_{z2})$. This spatial multilayered structure has been used to create hyperbolic and epsilon near-zero metamaterials [14, 53] and has been applied to different scenarios such as focusing devices [58, 59], demonstrating a successful mechanism to achieve tailored electromagnetic parameters. This technique has been developed within the frequency domain by using different materials in the spatial coordinates. However, an interesting question may be asked: would it be possible to design metamaterials using such techniques in the time domain? More specifically, would it be possible to achieve an arbitrary tailored effective permittivity by simply modulating the permittivity of the entire (spatially unbounded) medium in time, much faster than the frequency of the signal?

To answer this question, let us discuss the relation and analogy between the spatial multilayered metamaterial and the proposed temporal scenario shown in Figure 1A and C, respectively. For the temporal case shown in Figure 1C, we have considered a monochromatic wave traveling in a spatially unbounded medium with the relative permeability $\mu = 1$ and a time-dependent relative permittivity $\varepsilon(t)$. This $\varepsilon(t)$ is temporally changed between ε_1 and ε_2 (both positive real quantities) with a period much smaller than the period of the incident wave. The aim here is to relate this temporal multistepped structure to a temporally effective permittivity initiated with a step function in time [as shown in Figure 1D]. A single step change of permittivity has been a research topic since the last century [32, 33]. It has been shown that with such temporal change of permittivity the wavenumber $\boldsymbol{k}$ is preserved while the frequency is modified from ω_1 to $\omega_2 = \left(\sqrt{\varepsilon_1}/\sqrt{\varepsilon_2}\right)\omega_1$ (with $\mu_1 = \mu_2$). Moreover, the temporal boundary created at the time of the rapid change[1] of ε is able to produce a forward and a backward wave with the latter traveling with the same angle, but opposite direction of the incident wave [32]. Interestingly, these exciting features have been shown to be equivalent of the "reflection" and "transmission", but in the time domain [60, 61]. Such temporal metamaterial has been used for different applications such as time reversal and frequency conversion [62].

By comparing Figure 1A,B and Figure 1C,D, a relation between the spatial and temporal multilayered/multistepped scenarios can be observed. Both cases have similar features such as the subwavelength thickness and subperiod temporal change of permittivity, respectively. The main difference relies on the fact that for the temporal case, frequency conversion and unaltered wavelength are expected (conservation of $\boldsymbol{k}$, i.e. the frequency changes while the wavelength stays unchanged) while for the spatial scenario the frequency remains the same while the wavelength is changed. However, as it will be discussed in the following, both spatial and temporal multilayers/multisteps share the analogous feature: the ability to create a metamaterial with an effective value of ε_{eff}.

To evaluate the performance of the proposed temporal multistepped metamaterial, let us consider a time-dependent permittivity with a step function, as shown in Figure 2A,B. Here, the permittivity of the whole medium is rapidly changed (with a rise/fall time much smaller than the period of the incident wave) from $\varepsilon_1 = 1$ to $\varepsilon_2 = 1.25$ and is kept at this value. With this setup, the numerical results[2] of the electric field for the forward wave at a single spatial location within the spatially unbounded medium (right-most position of a $20\lambda_1$ simulation box with $\lambda_1 = 0.2$ mm [$f_1 = 1.5$ GHz] as the wavelength of the incident monochromatic wave, see method Section for more details of the numerical model) are shown, as the green curve in Figure 2C, where it can be seen how the period of the signal after the permittivity change, i.e. (1.11T), is different from the one before the change of permittivity, i.e. (T), as expected due to the frequency change produced at the temporal boundary. Moreover, note that the amplitude of the electric field after the permittivity change is reduced from 1 to ~0.85. These results are in agreement with the

1 By "rapid change" we mean for the change not to be instantaneous, but fast enough to have the transient rise/fall time less than the period of the wave. Moreover, we consider the frequency of operation to be far from any material resonances and therefore the positive permittivity functions can be approximately assumed to be "non-dispersive".

2 In the numerical simulations by COMSOL Multiphysics® utilized here, the dispersion of the permittivity is justifiably ignored, as argued in the footnote (1).

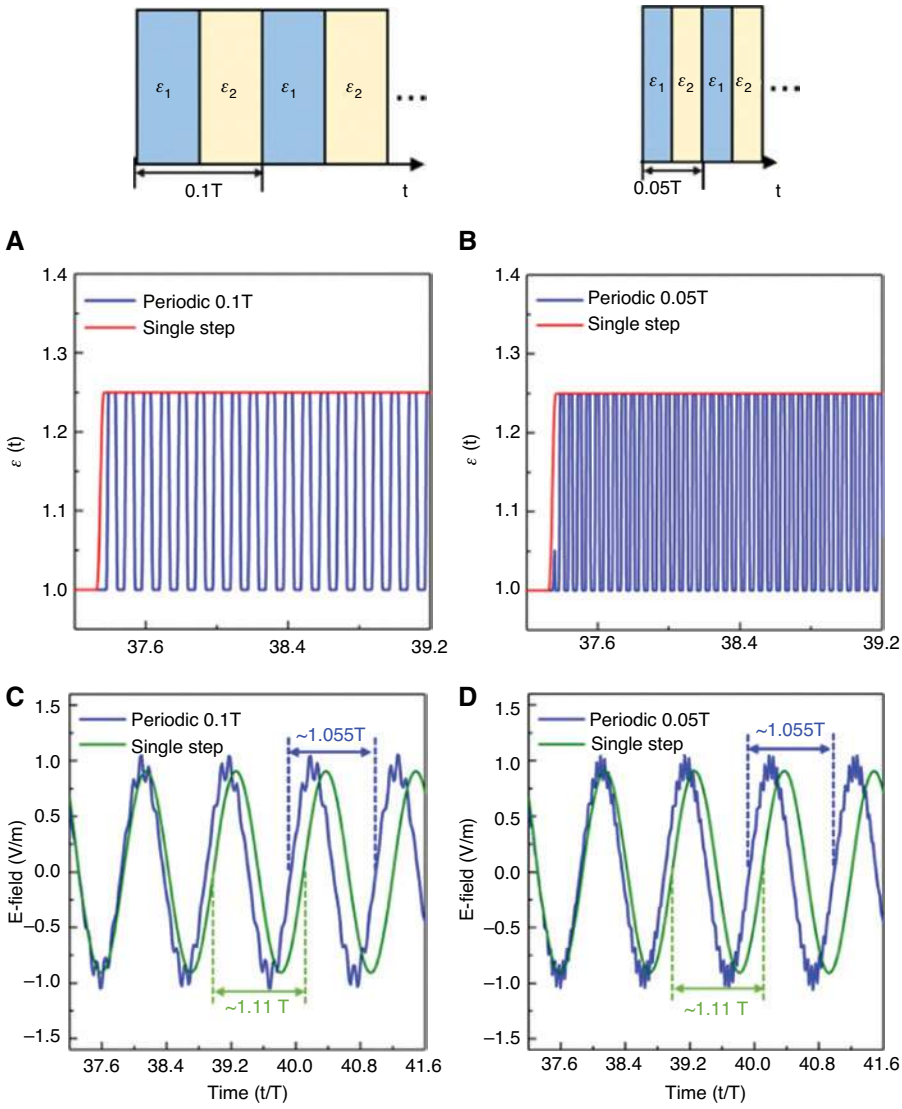

Figure 2: E-field using temporal multistepped ε(t) (alternating between ε_1 and ε_2) and a single step of ε(t) (from ε_1 to $\varepsilon_{eff}=\varepsilon_2$). (A, B) ε(t) considering a single step function that is changed from 1 to 1.25 (red lines) and a multistepped temporally periodic ε(t) changing between 1 and 1.25 with a periodicity of (1/10)T (blue line in A) and (1/20)T (blue line in B). (C, D) Simulation results for the electric field at a single location in the spatially unbounded medium for the single step function (green lines) of changing permittivity from 1 to 1.25, and a temporally periodic ε(t) changing from 1 to 1.25 with a periodicity of (1/10)T (blue line in C) and (1/20)T (blue line in D). The schematic representations of the temporal multistepped metamaterial for each case are shown in the first row.

expected change of the E field at the temporal boundary in the time domain [33] where an amplitude of the electric field of 0.85 is theoretically predicted when the permittivity is modified from 1 to 1.25. Note that in these results we are only plotting the field distribution for the forward wave, but a backward wave is also excited once inducing the temporal boundary. However, since the change of permittivity is small ($\varepsilon_1=1$ to $\varepsilon_2=1.25$ for a step function of permittivity) the "temporal equivalent" of Fresnel coefficient for this backward wave $R=0.5\left[(\varepsilon_1/\varepsilon_2)-\left(\sqrt{\varepsilon_1}/\sqrt{\varepsilon_2}\right)\right]$ [32, 33, 63] is almost negligible with a value of −0.047. From now on we will show the results of the generated forward wave and a discussion regarding the backward waves will be presented in Section 2.3.

Now, what if we use a temporally periodic permittivity, i.e. rapidly alternating it between 1 and 1.25? To evaluate this scenario, we can consider the time-dependent permittivities shown in Figure 2A,B as blue lines with a periodicity of (1/10)T and (1/20)T, respectively. A schematic representation of the periodic change is shown in the first row of Figure 2 to guide the eye. With this configuration, the numerical results of the electric field distribution at the same location as that of the single step

function are shown in Figure 2C,D. As observed, the electric field distribution for the temporally periodic multistepped metamaterial present some "ripples" which can be explained as follows: when the permittivity is first changed from $\varepsilon_1=1$ to $\varepsilon_2=1.25$, the amplitude of the temporal E field is modified to a value that can be calculated using the "temporal equivalent" of the Fresnel coefficient for the forward wave $T_1=0.5\left[(\varepsilon_1/\varepsilon_2)+\left(\sqrt{\varepsilon_1}/\sqrt{\varepsilon_2}\right)\right]$ [32, 33, 63]. i.e. the amplitude is reduced because $\varepsilon_2>\varepsilon_1$. Now, when the permittivity is returned to its initial value (from $\varepsilon_2=1.25$ to $\varepsilon_1=1$) the amplitude of the temporal E field will be increased following $T_2=0.5\left[(\varepsilon_2/\varepsilon_1)+\left(\sqrt{\varepsilon_2}/\sqrt{\varepsilon_1}\right)\right]$. Hence, the "ripples" are produced due to the fact that the temporal E field will experience multiple changes in its amplitude, because of the multiple temporal boundaries induced in the periodic scenario. Moreover, such E field possesses higher frequency harmonics (as it will be further discussed in the following Sections), but our interest is mostly on its fundamental frequency. By comparing these results with those obtained with the single step function, we can see how the period (and hence the frequency) of the wave for the temporally periodic change of permittivity is different from that of the single step change of ε with a clear mismatch between the results. Moreover, note that the period of the wave for the case with a step function of permittivity is longer (1.11T) compared to the temporal multistepped cases (~1.055T). This implies that the new frequency of the wave with the temporally periodic $\varepsilon(t)$ is actually higher than the one produced when using a single step change of ε in time from 1 to 1.25.

Based on these results, in order to match the converted frequency of the temporal multisteps with that of the single change of permittivity in time, it is necessary to modify the value ε_2 for the case of the single step change to a value ε_{eff} smaller than that used for ε_2 in the temporal multistepped case. By doing this, the converted frequency of the single step change of permittivity will be increased (see previous discussion about the frequency conversion at the temporal boundary) and the period of the converted wave will match that of the temporal multistepped metamaterial. But, what should be the value of ε_{eff} for such single step change? The answer to this question can be obtained by exploiting the similarities between the spatial multilayered metamaterial Eq. (1) and the temporal multistepped scenario: it can be suggested that the temporally effective permittivity created by the latter case would be equivalent to a step function with a single temporal change of permittivity from ε_1 to ε_{eff} such that ε_{eff} for the step function will be an "effective" value between the ε_1 and ε_2 used for the temporal multistepped case. Hence, the temporally effective permittivity can be expressed as follows (the analytical derivation can be found in the methods section below):

$$\varepsilon_{\text{eff}}=\frac{\varepsilon_1\varepsilon_2}{\varepsilon_1\Delta t_2+\varepsilon_2\Delta t_1} \tag{2}$$

where $\Delta_{t1}=1-\Delta_{t2}$ and Δ_{t2} are the filling fractions (in time) for each temporal step (times where the permittivity is ε_1 and ε_2, respectively).

By comparing Eq. (1b) and Eq. (2) it can be seen how the temporal and spatial multistepped/multi-layererd metamaterials are connected with a similar expression for the effective permittivity in both domains. This duality can also be seen in terms of the boundary conditions for the spatial and temporal scenarios: in the former case, the $\varepsilon_{\text{effzz}}$ defined by Eq. (1b), the normal component of vector $\boldsymbol{D}$ is preserved at each spatial interface between the two materials with ε_1 and ε_2. Similarly, in the temporal scenario, $\boldsymbol{D}$ should be preserved at each temporal boundary produced when the permittivity is rapidly changed from ε_1 to ε_2 [32, 33, 41, 42].

To evaluate and test Eq. (2), the numerical results of the electric field distribution at the same location as Figure 2 for both temporal multistepped metamaterials with period (1/10)T and (1/20)T with $\Delta_{t1}=\Delta_{t2}=0.5$ are shown in Figure 3B,D along with the results using a single step function for ε_{eff} following Eq. (2), with $\varepsilon_1=1$ and $\varepsilon_{\text{eff}}=1.111$. Note that the results for the temporal multisteps are those also shown in Figure 2C,D, but are re-plotted here for a better comparison. From these results, it can be clearly seen how similarity is achieved between the periodicity of the wave for the case of a single step change of permittivity and that obtained using the temporally periodic case.

For the sake of completeness, the results of the electric field at the same location as before considering a temporal multistepped metamaterial with a period of 0.4T are shown in Figure 3F and the time-dependent permittivity for this case is shown in Figure 3E. By comparing these results with those using smaller periods (such as 0.1T and 0.05T), the good matching with the single step change is not achieved. This is expected because the effective permittivity described in Eq. (2) is valid for periods much smaller than the period of the incident wave (an analogous feature holds for the spatial scenario where Eq. (1) is valid for layers with subwavelength thicknesses [53]). These results demonstrate that temporal multistepped metamaterials can produce a temporally effective permittivity (similar to the case of a spatial multilayer metamaterial) which can be modeled as a single step change of permittivity in time.

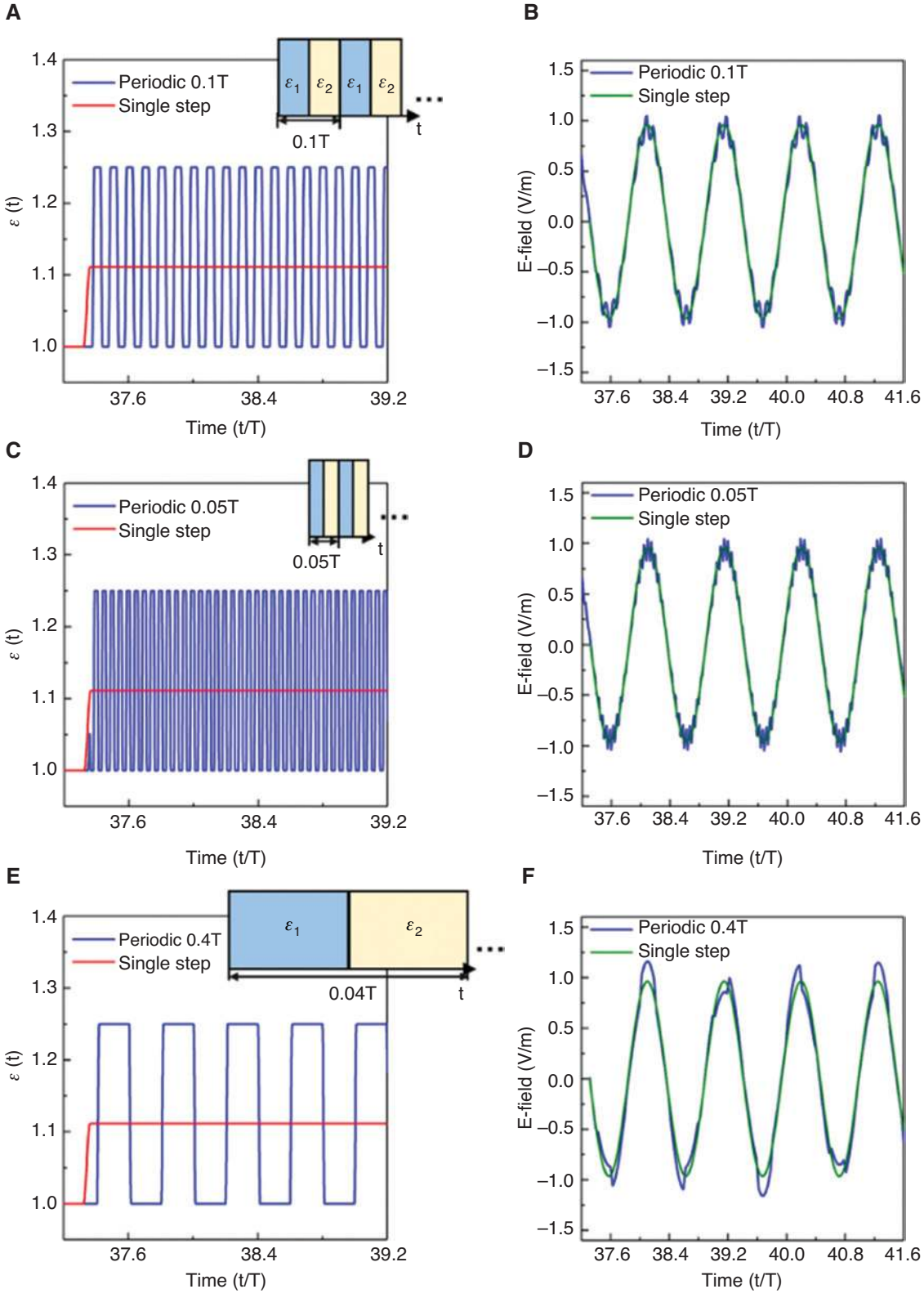

Figure 3: E-field using temporal multistepped ε(t) (alternating between ε_1 and ε_2) and a single step of ε(t) using Eq. (2). (A, C, E) ε(t) considering a single step function that is changed from 1 to $\varepsilon_{eff} = 1.111$ (red lines) and a temporally periodic ε(t) changing from 1 to 1.25 with a periodicity of (1/10)T (blue line in A), (1/20)T (blue line in C) and (0.4)T (blue line in E). (B, D, F) Simulation results for the electric field of the forward wave at a single location for the single step function (green lines) and a temporally periodic ε(t) changing from 1 to 1.25 (blue lines) considering a periodicity of (1/10)T (B), (1/20)T (D) and (0.4)T (F). The schematic representations of the temporal multistepped metamaterial for each case are shown as insets in the first column.

2.2 Tailoring the temporal effective permittivity

To further study the performance of the temporal multistepped metamaterial, we put forward the following question: would it be possible to tailor the effective permittivity to any arbitrary value between the two positive ε_1 and ε_2? As is known, this can be achieved with the spatial multilayered case by simply changing the filling fraction of the two materials used for each of the layers [14], see Eq. (1a,b). Hence, since the proposed temporal multistepped metamaterial is the dual of the spatial case described by Eq. (1b), one can also tailor the effective permittivity in the time domain by changing the temporal filling fraction for each temporal layer (Δ_{t1} and Δ_{t2}) in Eq. (2).

To verify this, the numerical results of the electric field using different values of duty cycle (DC) ranging from 0.2 to 0.8 with a period of (1/10)T for the temporally periodic permittivity of the temporal multisteps are shown in the third row of Figure 4. Here, a DC of 0.2 and 0.8 mean $\Delta_{t2}=0.2\times0.1\mathrm{T}$ and $\Delta_{t2}=0.8\times0.1\mathrm{T}$, respectively. The temporally periodic permittivities for each case are shown in the first and second rows of Figure 4. As observed, the period (and hence the effective permittivity) of each case is changed depending on the value of DC used. To better observe this performance, the effective permittivity for each case can be calculated using Eq. (2) and the resulting single step functions for each DC are plotted as red curves in the second row of Figure 4. It is shown for a DC of 0.2, 0.4, 0.6 and 0.8 the effective permittivity is equivalent to a single step function that is rapidly changed from 1 to $\varepsilon_{\mathrm{eff}}$ of 1.041, 1.087, 1.136 and 1.190, respectively. With these parameters, the numerical results for the electric field distribution using each effective step function of permittivity are shown as green curves in the third row of Figure 4. As observed, an excellent agreement is obtained between the results, demonstrating how the temporal multistepped metamaterial can be used to create an arbitrary temporally effective permittivity between ε_1 and ε_2 by simply changing the DC.

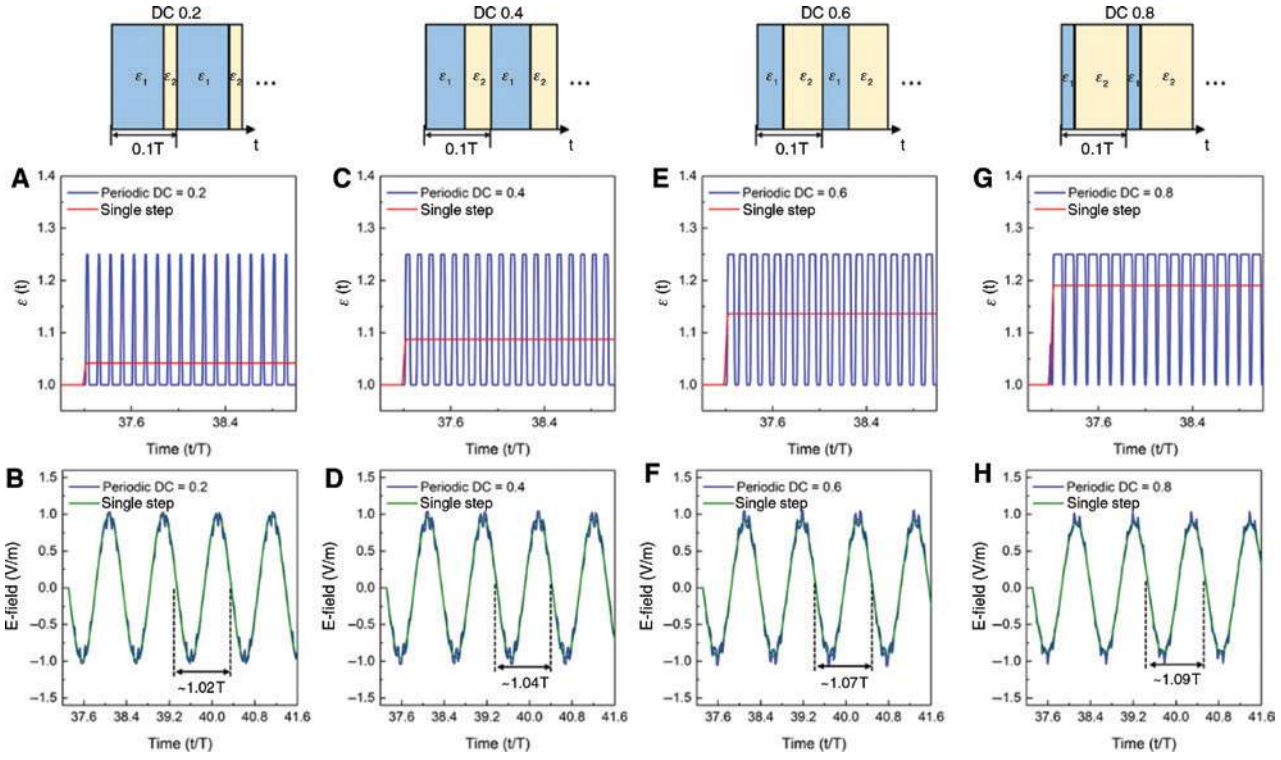

Figure 4: Effect of changing the duty cycle.
(A, C, E, G) $\varepsilon(t)$ considering a single step function (red lines) that is changed from 1 to $\varepsilon=1.041$ (A), 1.087 (C), 1.136 (E) and 1.190 (G) along with the temporally periodic $\varepsilon(t)$ (blue lines) changing from 1 to 1.25 with a periodicity of (1/10)T and a duty cycle (DC) of 0.2 (A), 0.4 (C), 0.6 (E) and 0.8 (G). (B, D, F, H) Simulation results for the electric field of the forward wave at a single location for the single step function (green lines) and temporally periodic $\varepsilon(t)$ (blue lines) considering the permitivities shown in panels (A, C, E, G) with a duty cycle of 0.2 (B), 0.4 (D), 0.6 (F) and 0.8 (H). The schematic representations of the temporal multistepped metamaterials for each case are shown in the first row.

2.3 Results for higher values of ε_2

In the previous sections, the temporal multistepped scenario was demonstrated by periodically changing the permittivity between the two values of $\varepsilon_1=1$ to $\varepsilon_2=1.25$. To better appreciate the role of these values, here we give another example with higher $\varepsilon_2=2$ in order to evaluate a bigger change of permittivity. The total duration of each periodic multistep is the same as in the previous studies and two different DCs are considered (0.2 and 0.8) in order to further study the effect of the filling fraction in the temporal ε_{eff}.

With this configuration the numerical results of the electric field distribution considering a time-dependent permittivity rapidly changing between $\varepsilon_1=1$ to $\varepsilon_2=2$ are shown as blue lines in Figure 5B,F considering a DC of 0.2 and 0.8, respectively. These results are then compared with those obtained considering a time-dependent permittivity using a single step with effective permittivity calculated using Eq. (2) ($\varepsilon_{\text{eff}}=1.111$ for a duty cycle of 0.2 and $\varepsilon_{\text{eff}}=1.667$ for a duty cycle of 0.8). For completeness the time-dependent permittivity functions in both cases are shown in the Figure 5A,E for both duty cycles.

As observed, a good agreement is achieved between the results of the temporal multistepped metamaterials and the single steps, demonstrating the capability of using such temporal multisteps as an effective medium in the time domain. Moreover, note that the amplitude of the electric field for the case with a DC of 0.8 (~0.72 in Figure 5F) is smaller than the one obtained with a DC of 0.2 (~0.95 Figure 5B). As explained before, these are expected results because of the temporal coefficient for the electric field after the temporal change which theoretically predicts an amplitude of the electric field of ~0.7 and ~0.92 for a DC of 0.8 and 0.2, respectively. Moreover, we also note higher "ripples" in the E field, again expected due to the fact that the permittivity undergoes higher changes between 1 and 2, as explained in the previous sections. For completeness, the results of the normalized spectral contents calculated from the temporal E field from Figure 5B,F are shown in Figure 5C,G for DC values of 0.2 and 0.8, respectively. As it is shown, the ripples observed

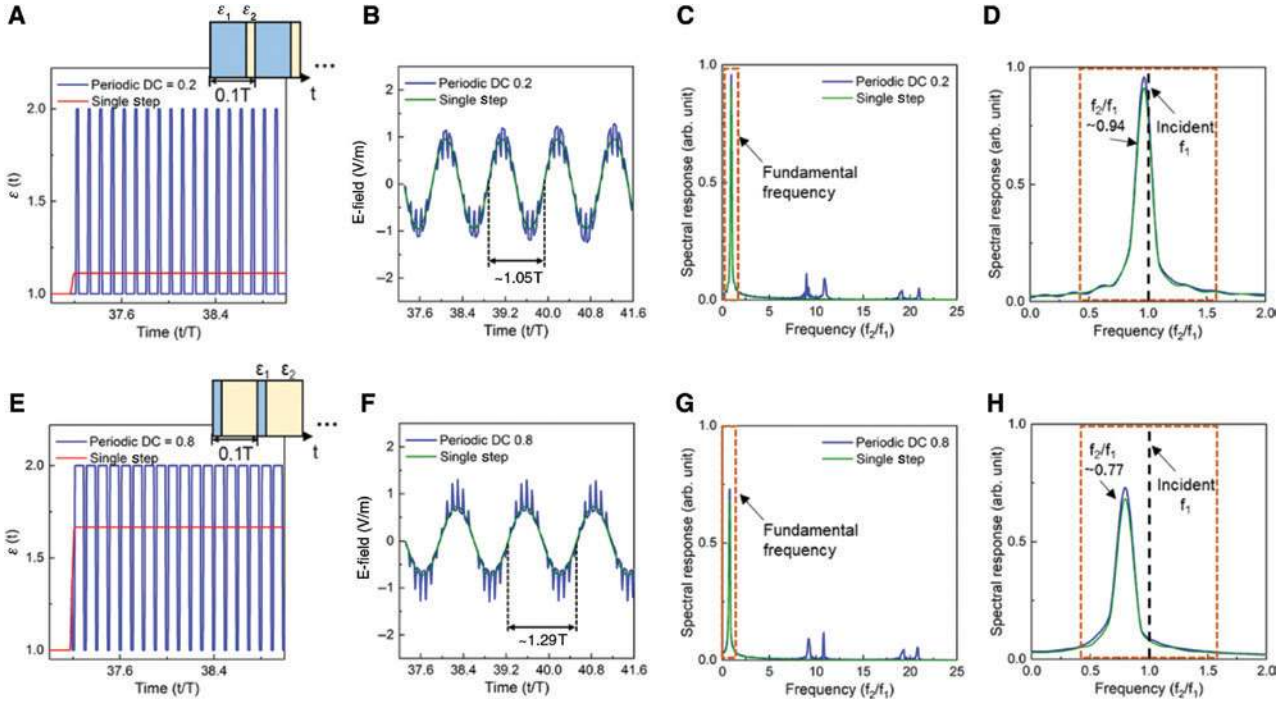

Figure 5: E-field distribution considering larger values of ε_2.
Similar to Figure 4 but with higher ε_2: (A, E) $\varepsilon(t)$ considering a single step function (red lines) that is changed from 1 to $\varepsilon_{\text{eff}}=1.111$ (A) and 1.667 (E) along with the temporally periodic $\varepsilon(t)$ (blue lines) changing from 1 to 2 with a periodicity of (1/10)T and a duty cycle (DC) of 0.2 (A) and 0.8 (E). (B, F) Simulation results for the electric field at a single location for the single step function (green lines) and temporally periodic $\varepsilon(t)$ (blue lines) considering the permitivities shown in panels (A, E) with a duty cycle of 0.2 (B) and 0.8 (F). (C, G) Normalized spectral response calculated from panels (B, F) considering a DC of 0.2 (C) and 0.8 (G), respectively. (D, H) Zoom-in of the normalized spectral response extracted from panels (C, G) showing the frequency change produced by the effective temporal effective medium. The schematic representations of the temporal multistepped metamaterials for each case are shown as the insets in the first column where the blue and yellow blocks represent $\varepsilon_1=1$ and $\varepsilon_2=2$, respectively. The electric field in this figure correspond to that of the forward wave.

in the time domain (Figure 5B,F) are translated into higher-order harmonics, as discussed before. However, note that their amplitude is much smaller than that of the fundamental frequency demonstrating that the temporal effective medium is still valid (for the fundamental frequency) in temporal multistepped metamaterials for cases when the change of permittivitty is increased. For completeness, a zoom-in of the spectral contents around the fundamental harmonic extracted from Figure 5C,G is shown in Figure 5D,H, respectively. As observed, a good agreement is again noticeable between the results of the temporal multisepped metamaterial and the effective temporal medium modeled as a single step. From these results, the frequency is changed from f_1 to $f_2 \approx 0.94 f_1$ and to $f_2 \approx 0.77 f_1$ when using a DC of 0.2 and 0.8, respectively, in agreement with theoretical calculations [32] which predict a frequency change of $f_2 \approx 0.948 f_1$ and $f_2 \approx 0.774 f_1$ for each DC, respectively.

In all the results discussed in the previous section (Figures 2–5) we have shown the results of the distribution of the temporal E field of the forward wave (FW) at a single location. However, since we have demonstrated how the multistepped temporal metamaterial is able to emulate an effective permittivity as if the permittivity was changed in time using a single step function, it is important to show that a backward wave (BW) is also produced for the case when such a multistepped temporal metamaterial is implemented.

To do this, let us consider a multistepped temporal metamaterial with a time-dependent permittivity that is initially $\varepsilon_1 = 2$ and then it is periodically changing between $\varepsilon_1 = 2$ and $\varepsilon_2 = 1$. The results of the spatial distribution of the electric field at different times are shown in Figure 6 considering a DC of 0.2 (Figure 6A,B) and 0.8 (Figure 6C,D). The field distribution using the multistepped temporal metamaterials are shown in Figure 6A,C along with their effective medium using a single step of permittivity, Figure 6B,D. From these results a good agreement is observed for the field distribution of the multistepped temporal metamaterials resembling the one generated by their effective version using a single step. Moreover, note that the BW wave is created in all the cases shown in Figure 6 with their spatial distributions showing the same wavelength as the FW waves, i.e. after the temporal change of permittivity, k remains the same while the frequency is changed. Finally, note that the BW is more evident for the case with DC = 0.8 which is due to the fact that the effective permittivity ($\varepsilon_{\text{eff}} = 1.111$) is smaller than the one produced with a DC of 0.2 ($\varepsilon_{\text{eff}} = 1.667$). Hence, it is expected to have a larger amplitude for the BW wave when the permittivity is effectively changed in a single step from ε_1 to $\varepsilon_{\text{eff}} = 1.111$ since $R = 0.5\left[(\varepsilon_1 / \varepsilon_{\text{eff}}) - \left(\sqrt{\varepsilon_1} / \sqrt{\varepsilon_{\text{eff}}}\right)\right]$ [32, 33].

Such multistepped temporal metamaterials could be realized at microwave frequencies by using circuit elements loaded in transmission lines [64] in order to change the permittivity between two different values. This can become more challenging when working at higher frequencies (such as the IR and visible spectrum) due to the reduced period of the signal. However, within the past few years great efforts have been devoted to rapidly tuning the electromagnetic properties of materials at optical frequencies. In this realm, the frequency conversion using temporal boundaries has been recently demonstrated experimentally at such spectral range [37, 65]. Hence, we are optimistic that our concept of multistepped temporal metamaterials as a way to produce an effective temporal permittivity could be realized not just at microwaves, but at higher frequencies in the near future.

3 Methods

3.1 Analytical solution for the effective permittivity in temporal multisetpped metamaterials

As explained in the Introduction, the interaction of electromagnetic waves with time-dependent media has gained much attention in the scientific community. In this realm, time-dependent periodic metamaterials have been recently studied demonstrating their capability to achieve the temporal version of a photonic band-gap structure by using different functions of permittivity and/or permeability [41, 42, 66]. Here, we focused our attention in the analytical formulation of the effective permittivity for the temporal scenario analogous with the spatial multilayered metamaterial using the transfer matrix method. The structure under study is the one shown in Figure 1C,D.

Based on the transfer matrix method, each temporal step in the multistep scenario from Figure 1C can be defined by a characteristic matrix, as follows [67]:

$$M_j(\tau_j) = \begin{bmatrix} a_{11} & a_{12} \\ a_{21} & a_{22} \end{bmatrix}; \; j = 1,2, \tag{3}$$

where j represents each temporal multistep with permittivity ε_1 and ε_2, respectively. In this realm, because (a) the change of permittivity is applied to the whole medium where the wave is traveling (unbounded medium) and (b) the wavenumber k is preserved at each temporal

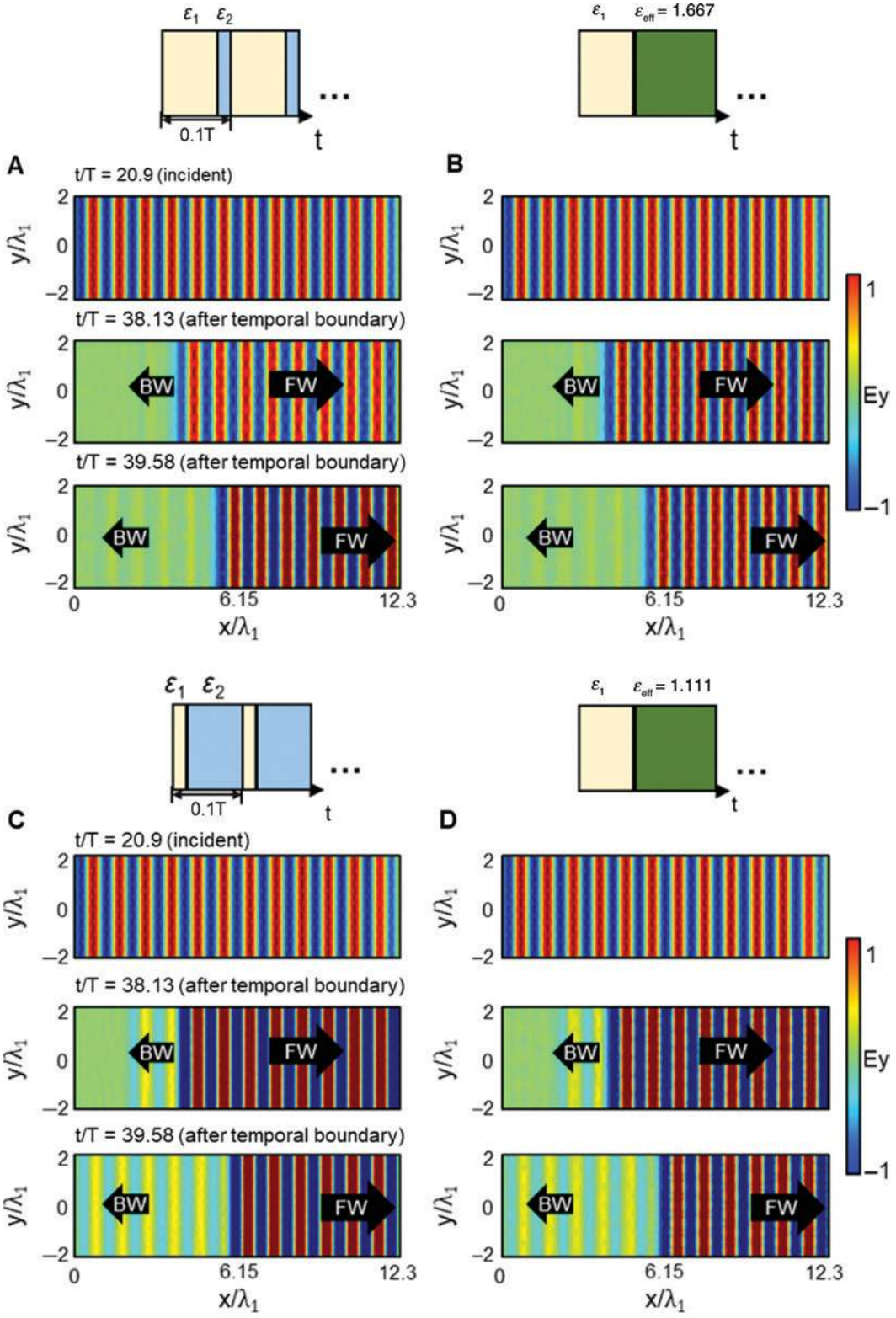

Figure 6: Spatial distribution of the electric field at different times considering a time-dependent permittivity with an initial value of $\varepsilon_1 = 2$. The permittivity is then changed periodically (between $\varepsilon_1 = 2$ and $\varepsilon_2 = 1$) or in a single step (from $\varepsilon_1 = 2$ to ε_{eff}) at the normalized time t/T = 37.3 (as in Figures 2–5): (A, C) Using a temporally periodic $\varepsilon(t)$ changing from 2 to 1 with a periodicity of (1/10)T and a duty cycle (DC) of 0.2 (A) and 0.8 (C). (B, D) A single step function that is changed from 2 to $\varepsilon_{eff} = 1.667$ (B) and $\varepsilon_{eff} = 1.111$ (D). For these results, the incoming signal is switched off once the first temporal boundary is induced in order to better appreciate the FW and BW waves created with both multistepped temporal metamaterial and its effective equivalent version using a single step metamaterial. Note that the color bars have been saturated from –1 to 1 to better appreciate the BW waves.

boundary [32] the characteristic matrix for the temporal multisteps in Figure 1C can be then calculated as follows:

$$M_1(\tau_1)=\begin{bmatrix}\cos(\omega_1\tau_1) & -\frac{i}{\sqrt{\varepsilon_1}}\sin(\omega_1\tau_1)\\ -i\sqrt{\varepsilon_1}\sin(\omega_1\tau_1) & \cos(\omega_1\tau_1)\end{bmatrix} \tag{4a}$$

$$M_2(\tau_2)=\begin{bmatrix}\cos(\omega_2\tau_2) & -\frac{i}{\sqrt{\varepsilon_2}}\sin(\omega_2\tau_2)\\ -i\sqrt{\varepsilon_2}\sin(\omega_2\tau_2) & \cos(\omega_2\tau_2)\end{bmatrix} \tag{4b}$$

where τ_1 and τ_2 are the absolute temporal duration of each multistep. The total period of the multistep is then $\tau_{\text{total}}=\tau_1+\tau_2<<\text{T}$. As the result, the filling factors (Δ_{t1} and Δ_{t2}) in Eq. (2) are $\Delta_{t1}=\tau_1/\tau_{\text{total}}$ and $\Delta_{t2}=\tau_2/\tau_{\text{total}}$. As observed, Eqs. (4a,b) only depend on the frequencies at each temporal step $\omega_{1,2}$ and their absolute temporal duration $\tau_{1,2}$, meaning that each induced temporal step does not affect the spatial distribution of the wave since its wavelength is not modified (conservation of k).

Now, we can calculate an equivalent matrix $M(\tau_{\text{total}})$ for the whole period τ_{total} by simply multiplying Eqs. (4a,b). Based on this, $M(\tau_{\text{total}})$ can be expressed in the following manner:

$$M(\tau_{\text{total}})=M_1(\tau_1)M_2(\tau_2)=\begin{bmatrix}a_{11\text{total}} & a_{12\text{total}}\\ a_{21\text{total}} & a_{22\text{total}}\end{bmatrix} \tag{5a}$$

$$a_{11\text{total}}=\cos(\omega_1\tau_1)\cos(\omega_2\tau_2)-\frac{\sqrt{\varepsilon_2}}{\sqrt{\varepsilon_1}}\sin(\omega_1\tau_1)\sin(\omega_2\tau_2) \tag{5b}$$

$$a_{12\text{total}}=-i\frac{1}{\sqrt{\varepsilon_2}}\cos(\omega_1\tau_1)\sin(\omega_2\tau_2)-i\frac{1}{\sqrt{\varepsilon_1}}\sin(\omega_1\tau_1)\cos(\omega_2\tau_2) \tag{5c}$$

$$a_{21\text{total}}=-i\sqrt{\varepsilon_1}\sin(\omega_1\tau_1)\cos(\omega_2\tau_2)-i\sqrt{\varepsilon_2}\cos(\omega_1\tau_1)\sin(\omega_2\tau_2) \tag{5d}$$

$$a_{22\text{total}}=-\frac{\sqrt{\varepsilon_1}}{\sqrt{\varepsilon_2}}\sin(\omega_1\tau_1)\sin(\omega_2\tau_2)+\cos(\omega_1\tau_1)\cos(\omega_2\tau_2) \tag{5e}$$

Now we can define a characteristic matrix for an equivalent medium made of an effective permittivity (ε_{eff}) as follows:

$$M_{\text{eff}}(\tau_{\text{total}})=\begin{bmatrix}a_{11\text{eff}} & a_{12\text{eff}}\\ a_{21\text{eff}} & a_{22\text{eff}}\end{bmatrix} \tag{6a}$$

$$M_{\text{eff}}(\tau_{\text{total}})=\begin{bmatrix}\cos(\omega_{\text{eff}}\tau_{\text{total}}) & -\frac{i}{\sqrt{\varepsilon_{\text{eff}}}}\sin(\omega_{\text{eff}}\tau_{\text{total}})\\ -i\sqrt{\varepsilon_{\text{eff}}}\sin(\omega_{\text{eff}}\tau_{\text{total}}) & \cos(\omega_{\text{eff}}\tau_{\text{total}})\end{bmatrix} \tag{6b}$$

with ω_{eff} as the effective angular frequency of the equivalent medium. Based on this, the equivalent medium described by the equation above will be the same as the one defined by Eq. (5) by defining the equalities between each element of both matrices: $a_{11\text{total}}=a_{11\text{eff}}$, $a_{12\text{total}}=a_{12\text{eff}}$, $a_{21\text{total}}=a_{21\text{eff}}$ and $a_{22\text{total}}=a_{22\text{eff}}$. After applying these equivalences between Eqs. (5–6), the effective permittivity can then be extracted using the following equality between both characteristic matrices:

$$a_{12\text{total}}=a_{12\text{eff}} \tag{7a}$$

$$\frac{-i}{\sqrt{\varepsilon_2}}\cos(\omega_1\tau_1)\sin(\omega_2\tau_2)-\frac{i}{\sqrt{\varepsilon_1}}\sin(\omega_1\tau_1)\cos(\omega_2\tau_2)=-\frac{i}{\sqrt{\varepsilon_{\text{eff}}}}\sin(\omega_{\text{eff}}\tau_{\text{total}}) \tag{7b}$$

where $=\tau_1$ and $\tau_2<<\text{T}$, $\omega_2=(\sqrt{\varepsilon_1}/\sqrt{\varepsilon_2})\omega_1$ and $\omega_{eff}=(\sqrt{\varepsilon_1}/\sqrt{\varepsilon_{\text{eff}}})\omega_1$. Based on this, Eq. (7b) is reduced to:

$$-\frac{i}{\sqrt{\varepsilon_2}}\omega_2\tau_2-\frac{i}{\sqrt{\varepsilon_1}}\omega_1\tau_1=-\frac{i}{\sqrt{\varepsilon_{\text{eff}}}}\omega_{\text{eff}}\tau_{\text{total}} \tag{7c}$$

$$\frac{\tau_2}{\varepsilon_2}+\frac{\tau_1}{\varepsilon_1}=\frac{\tau_{\text{total}}}{\varepsilon_{\text{eff}}} \tag{7d}$$

$$\varepsilon_{\text{eff}}=\frac{\varepsilon_1\varepsilon_2}{\varepsilon_1\Delta t_2+\varepsilon_2\Delta t_1} \tag{7e}$$

Retrieving the expression shown in Eq. (2).

3.2 Simulation setup

The numerical analysis shown in Figures 2–6 was carried out using the time-domain solver of the commercial software COMSOL Multiphysics®. A simulation box of $20\lambda_1\times4\lambda_1$ was implemented and the FW waves were recorded at the right-most location of this box ($x=20\lambda_1$, $y=0$). To avoid undesirable reflections, top and bottom perfect electric conductor (PEC) boundaries were used with the scattering boundary condition at the right boundary in all the simulations. The incident field was applied from the left boundary of the simulation box via a scattering boundary condition. A triangular mesh was implemented with

a minimum and maximum size of $0.13\times10^{-3}\lambda_1$ to ensure accurate results. The rapid changes of ε in all these studies were modeled by implementing rectangular analytical functions with smooth transitions using two continuous derivatives to ensure convergence in the calculations.

4 Conclusions

In this work, temporal multistepped metamaterials have been investigated in order to achieve an effective permittivity in the time domain. It has been shown how temporal multisteps can produce a temporally effective permittivity modeled and initiated with a single step function of change of permittivity in time. The analogy between the spatial and temporal multilayered/multistepped metamaterials have been presented demonstrating the relation between both temporal and spatial domains. Within this context, it has been shown how the effective permittivity of the temporal multistepped metamaterial can be arbitrarily engineered by simply changing the duty cycle of the temporally periodic permittivity. This performance has been related and analogous to the spatial multilayered scenario where the effective permittivity can be manipulated by changing the filling fraction of the two subwavelength materials used as building blocks of the multilayered structure. The proposed technique has been analytically derived and numerically evaluated demonstrating an excellent agreement with the designed parameters. The results presented here may be applied to the design of effective permittivities in the time domain and may open new paths in the study of the exciting phenomena that may be achieved by using temporal metamaterials.

Acknowledgement: The authors would like to acknowledge the partial support from the Vannevar Bush Faculty Fellowship program sponsored by the Basic Research Office of the Assistant Secretary of Defense for Research and Engineering and funded by the Office of Naval Research through grant N00014-16-1-2029, Funder Id: http://dx.doi.org/10.13039/100000006. V.P.-P. acknowledges support from the Newcastle University (Newcastle University Research Fellow).

References

[1] Kock WE. Metal-lens antennas. Proc IRE 1946;34:828–36.
[2] Torres V, Pacheco-Peña V, Rodríguez-Ulibarri P, et al. Terahertz epsilon-near-zero graded-index lens. Opt Express 2013;219:156–66.
[3] Torres V, Orazbayev B, Pacheco-Peña V, et al. Experimental demonstration of a millimeter-wave metalic ENZ lens based on the energy squeezing principle. IEEE Trans Antennas Propag 2015;63:231–9.
[4] Pacheco-Peña V, Engheta N, Kuznetsov SA, Gentselev A, Beruete M. Experimental realization of an epsilon-near-zero graded-index metalens at terahertz frequencies. Phys Rev Appl 2017;8:034036-1–10.
[5] Vesseur EJR, Coenen T, Caglayan H, Engheta N, Polman A. Experimental verification of n = 0 structures for visible light. Phys Rev Lett 2013;110:013902.
[6] Zhang S, Fan W, Panoiu NC, Malloy KJ, Osgood RM, Brueck SRJ. Experimental demonstration of near-infrared negative-index metamaterials. Phys Rev Lett 2005;95:137404-1–4.
[7] Lee SH, Choi M, Kim T-T. Switching terahertz waves with gate-controlled active graphene metamaterials. Nat Mater 2012;11:936–41.
[8] Solymar L, Shamonina E. Waves in metamaterials. New York: Oxford University Press, 2009.
[9] Chen HT, Padilla WJ, Zide JMO, Gossard AC, Taylor AJ, Averitt RD. Active terahertz metamaterial devices. Nature 2006;444:597–600.
[10] Della Giovampaola C, Engheta N. Digital metamaterials. Nat Mater 2014;13:1115–21.
[11] Pacheco-Peña V, Orazbayev B, Torres V, Beruete M, Navarro-Cía M. Ultra-compact planoconcave zoned metallic lens based on the fishnet metamaterial. Appl Phys Lett 2013;103:183507.
[12] Moitra P, Yang Y, Anderson Z, Kravchenko II, Briggs DP, Valentine J. Realization of an all-dielectric zero-index optical metamaterial. Nat Photonics 2013;7:1–5.
[13] Liberal I, Engheta N. Near-zero refractive index photonics. Nat Photonics 2017;11:149–58.
[14] Maas R, Parsons J, Engheta N, Polman A. Experimental realization of an epsilon-near-zero metamaterial at visible wavelengths. Nat Photonics 2013;7:907–12.
[15] Dolling G, Enkrich C, Wegener M, Soukoulis CM, Linden S. Simultaneous negative phase and group velocity of light in a metamaterial. Science 2006;312:892–4.
[16] Marqués R, Martín F, Sorolla M. Metamaterials with negative parameters: theory, design and microwave applications. Hoboken NJ: Wiley, 2008.
[17] Pendry JB. Negative refraction makes a perfect lens. Phys Rev Lett 2000;85:3966–9.
[18] Liberal I, Li Y, Engheta N. Reconfigurable epsilon-near-zero metasurfaces via photonic doping. Nanophotonics 2018;7:1117–27.
[19] Liberal I, Engheta N. The rise of near-zero-index technologies. Science 2017;358:1540–1.
[20] Shafiei F, Monticone F, Le KQ, et al. A subwavelength plasmonic metamolecule exhibiting magnetic-based optical Fano resonance. Nat Nanotechnol 2013;8:95–9.
[21] Rodríguez-Ulibarri P, Kuznetsov SA, Beruete M. Wide angle terahertz sensing with a cross-dipole frequency selective surface. Appl Phys Lett 2016;108:111104.
[22] Kabashin AV, Evans P, Pastkovsky S, et al. Plasmonic nanorod metamaterials for biosensing. Nat Mater 2009;8:867–71.
[23] Demetriadou A, Hao Y. Slim Luneburg lens for antenna applications. Opt Express 2011;19:19925–34.
[24] Soric JC, Engheta N, Maci S, AAlu S. Omnidirectional metamaterial antennas based on ε- near-zero channel matching. IEEE Trans Antennas Propag 2013;61:33–44.

[25] Orazbayev B, Beruete M, Navarro-Cía M. Wood zone plate fishnet metalens. EPJ Appl Metamaterials 2015;2:8.
[26] Lier E, Werner DH, Scarborough CP, Wu Q, Bossard JA. An octave-bandwidth negligible-loss radiofrequency metamaterial. Nat Mater 2011;10:216–22.
[27] Pacheco-Peña V, Torres V, Orazbayev B, et al. Mechanical 144 GHz beam steering with all-metallic epsilon-near-zero lens antenna. Appl Phys Lett 2014;105:243503.
[28] Ourir A, De Lustrac A. Metamaterial-based phased array for directional beam steering. Microw Opt Technol Lett 2009;51:2653–6.
[29] Pacheco-Peña V, Torres V, Beruete M, Navarro-Cia M, Engheta N. ε-near-zero (ENZ) graded index quasi-optical devices: steering and splitting millimeter waves. J Opt 2014;16:094009.
[30] Hashemi MRM, Yang SH, Wang T, Sepúlveda N, Jarrahi M. Electronically-controlled beam-steering through vanadium dioxide metasurfaces. Sci Rep 2016;6:1–8.
[31] Silva A, Monticone F, Castaldi G, Galdi V, Alù A, Engheta N. Performing mathematical operations with metamaterials. Sci (New York, NY) 2014;343:160–4.
[32] Fante RI. Transmission of electromagnetic waves into time-varying media. IEEE Trans Antennas Propag 1971;3:417–24.
[33] Morgenthaler F. Velocity modulation of electromagnetic waves. IRE Trans Microw Theory Tech 1958;6:167–72.
[34] Caloz C, Deck-Léger Z-L. Spacetime metamaterials. arXiv, 2019. arXiv:1905.00560v2.
[35] Huidobro PA, Galiffi E, Guenneau S, Craster RV, Pendry JB. Fresnel drag in space-time modulated metamaterials. Proc Natl Acad Sci 2019:1–6.
[36] Akbarzadeh A, Chamanara N, Caloz C. Inverse prism based on temporal discontinuity and spatial dispersion. Opt Lett 2018;43:3297–300.
[37] Preble SF, Xu Q, Lipson M. Changing the colour of light in a silicon resonator. Nat Photonics 2007;1:293–6.
[38] Torrent D, Poncelet O, Batsale JC. Nonreciprocal thermal material by spatiotemporal modulation. Phys Rev Lett 2018;120:125501.
[39] Nassar H, Xu XC, Norris AN, Huang GL. Modulated phononic crystals: non-reciprocal wave propagation and Willis materials. J Mech Phys Solids 2017;101:10–29.
[40] Estep NA, Sounas DL, Soric J, Alu A. Magnetic-free non-reciprocity and isolation based on parametrically modulated coupled-resonator loops. Nat Phys 2014;10:923–7.
[41] Zurita-Sánchez JR, Halevi P, Cervantes-González JC. Reflection and transmission of a wave incident on a slab with a time-periodic dielectric function (t). Phys Rev A – At Mol Opt Phys 2009;79:1–13.
[42] Martínez-Romero JS, Becerra-Fuentes OM, Halevi P. Temporal photonic crystals with modulations of both permittivity and permeability. Phys Rev A 2016;93:1–9.
[43] Bacot V, Labousse M, Eddi A, Fink M, Fort E. Time reversal and holography with spacetime transformations. Nat Phys 2016;12:972–7.
[44] Vezzoli S, Bruno V, DeVault C, et al. Optical time reversal from time-dependent Epsilon-Near-Zero media. Phys Rev Lett 2018;120:43902.
[45] Sivan Y, Pendry JB. Theory of wave-front reversal of short pulses in dynamically tuned zero-gap periodic systems. Phys Rev A – At Mol Opt Phys 2011;84:1–16.
[46] Salem MA, Caloz C. Wave propagation in periodic temporal slabs. In: 2015 9th European Conference on Antennas and Propagation (EuCAP), 2015. https://ieeexplore.ieee.org/document/7228592.
[47] Salem MA, Caloz C. Temporal photonic crystals: Causality versus periodicity. In: Proceedings of the 2015 International Conference on Electromagnetics in Advanced Applications, ICEAA 2015, 2015;1:490–3. DOI: 10.1109/ICEAA.2015.7297162.
[48] Lerosey G, De Rosny J, Tourin A, Derode A, Montaldo G, Fink M. Time reversal of electromagnetic waves. Phys Rev Lett 2004;92:193904.
[49] Shapere A, Wilczek F. Classical time crystals. Phys Rev Lett 2012;109:160402-1–4.
[50] Wilczek F. Quantum time crystals. Phys Rev Lett 2012;109:160401-1–5.
[51] Zhang J, Hess PW, Kyprianidis A, et al. Observation of a discrete time crystal. Nature 2017;543:217–20.
[52] Choi S, Choi J, Landig R, et al. Observation of discrete time-crystalline order in a disordered dipolar many-body system. Nature 2017;543:221–5.
[53] Cortes CL, Newman W, Molesky S, Jacob Z. Quantum nanophotonics using hyperbolic metamaterials. J Opt 2012;14:1–15.
[54] Chern R-L. Spatial dispersion and nonlocal effective permittivity for periodic layered metamaterials. Opt Express 2013;21:16514.
[55] Afinogenov BI, Popkova AA, Bessonov VO, Lukyanchuk B, Fedyanin AA. Phase matching with Tamm plasmons for enhanced second- and third-harmonic generation. Phys Rev B 2018;97:1–5.
[56] Sihvola A. Electromagnetic mixing formulas and applications. Herts, United Kingdom: The institution of Electrical Engineers (IET), 1999.
[57] Belov PA, Hao Y. Subwavelength imaging at optical frequencies using a transmission device formed by a periodic layered metal-dielectric structure operating in the canalization regime. Phys Rev B – Condens Matter Mater Phys 2006;73:1–4.
[58] Nielsen RB, Thoreson MD, Chen W, et al. Toward superlensing with metal–dielectric composites and multilayers. Appl Phys B 2010;100:93–100.
[59] Maas R, van de Groep J, Polman A. Planar metal/dielectric single-periodic multilayer ultraviolet flat lens. Optica 2016;3:592.
[60] Plansinis BW. Donaldson WR, Agrawal GP. What is the temporal analog of reflection and refraction of optical beams? Phys Rev Lett 2015;115:1–5.
[61] Xiao Y, Maywar DN, Agrawal GP. Reflection and transmission of electromagnetic waves at temporal boundary. Opt Lett 2014;39:577.
[62] Chumak AV, Tiberkevich VS, Karenowska AD, et al. All-linear time reversal by a dynamic artificial crystal. Nat Commun 2010;1:141–5.
[63] Pacheco-Peña V, Kiasat Y, Edwards B, Engheta N. Salient features of temporal and spatio-temporal metamaterials. In: 2018 International Conference on Electromagnetics in Advanced Applications (ICEAA), 2018:524–6. DOI: 10.1109/ICEAA.2018.8520356.
[64] Qin S, Xu Q, Wang YE. Nonreciprocal components with distributedly modulated capacitors. IEEE Trans Microw Theory Tech 2014;62:2260–72.
[65] Lee K, Son J, Park J, et al. Linear frequency conversion via sudden merging of meta-atoms in time-variant metasurfaces. Nat Photonics 2018;12:765–73.
[66] Koutserimpas TT, Fleury R. Electromagnetic waves in a time periodic medium with step-varying refractive index. IEEE Trans Antennas Propag 2018;66:5300–7.
[67] Abu El-Haija AJ. Effective medium approximation for the effective optical constants of a bilayer and a multilayer structure based on the characteristic matrix technique. J Appl Phys 2003;93:2590–4.